

# Impact of trapped particles on the plasma sheath around infinitely-long electron-emitting objects in Maxwellian plasmas

L. Chiabò<sup>1</sup>, G. Sánchez-Arriaga<sup>1</sup>, P. Resendiz Lira<sup>2</sup>, G.L. Delzanno<sup>2</sup>

<sup>1</sup>*Bioengineering and Aerospace Engineering Department, Universidad Carlos III de Madrid, Madrid, Spain*

<sup>2</sup>*T-5 Applied Mathematics and Plasma Physics, Los Alamos National Laboratory, Los Alamos (NM 87545), USA*

## Introduction

The kinetic description of the plasma sheaths around two-dimensional electron-emitting object has multiple applications ranging from spacecraft and dust charging problems to modeling of emissive probes and cathodic segments of Low Work-function Tethers. The trapping of charged particles inside the sheath can modify significantly the structure of the sheath and the macroscopic magnitudes of interest [1, 2, 3, 4, 5, 6, 7, 8, 9]. The present work implements three numerical tools to assess the impact of the population of trapped particles on the structure of the sheath: i) a *Stationary Vlasov-Poisson Solver* (SVPS) based on the Orbital Motion Theory (OMT) for the sheath around infinitely long cylinders [10], ii) a *PIC* code for plasma-material interface problems with *curvilinear* geometries (CPIC) [11], and iii) a *Non-Stationary Vlasov-Poisson Solver* (NSVPS) based on a backward semi-Lagrangian approach currently under development.

A parametric analysis varying the emission level is presented to quantify the influence of the trapped population on the onset of the Space Charge Limited (SCL) operational regime, which is known to bring simple analytical descriptions like the Orbital Motion Limited (OML) theory to provide inaccurate results [12].

## 2D model for emissive probes

A cylindrical probe of radius  $R_p$  is immersed at rest in a collisionless, unmagnetised, Maxwellian plasma with density  $n_0$  and temperature  $T_\alpha$ , with  $\alpha = e$  ( $\alpha = i$ ) identifying plasma electrons (ions). Half-Maxwellian electrons ( $\alpha = em$ ) with density  $n_{em0}$  are emitted at the probe contour  $\Gamma$ , which is biased at  $\phi_p$  with respect to the plasma. For convenience, we introduce the following normalisation

$$\frac{\mathbf{r}}{\lambda_{De}} \rightarrow \mathbf{r}, \quad \frac{\mathbf{v}}{\sqrt{2}v_{the}} \rightarrow \mathbf{v}, \quad \frac{n_{e,i}}{n_0} \rightarrow n_{e,i}, \quad \frac{n_{em}}{n_{em0}} \rightarrow n_{em}, \quad (1a)$$

$$\sqrt{2}\omega_{pe}t \rightarrow \tau, \quad \frac{2k_B T_\alpha f_\alpha}{m_\alpha n_{\alpha 0}} \rightarrow f_\alpha(\mathbf{r}, \mathbf{v}), \quad \frac{e\phi}{k_B T_e} \rightarrow \phi(\mathbf{r}), \quad (1b)$$

with  $\lambda_{De} \equiv \sqrt{(\epsilon_0 k_B T_e)/(n_0 e^2)}$  the electron Debye length,  $v_{the} \equiv \sqrt{k_B T_e/m_e}$  the thermal velocity of electrons,  $\omega_{pe} = \lambda_{De}/v_{the}$  the electron plasma frequency, being  $k_B$ ,  $\epsilon_0$  the Boltzmann constant and the electric permittivity of the vacuum. The sheath is governed by the Vlasov-Poisson (VP) system

$$\frac{\partial f_\alpha}{\partial \tau} + \mathbf{v}_\alpha \cdot \nabla_{\mathbf{r}} f_\alpha - \frac{e_\alpha}{2\mu_\alpha} \nabla \phi \cdot \nabla_{\mathbf{v}} f_\alpha = 0,$$

$$\Delta \phi = -\rho \equiv n_e + \beta n_{em} - e_i n_i, \quad n_\alpha(\tau, \mathbf{r}) = \int_{-\infty}^{+\infty} f_\alpha(\tau, \mathbf{r}, \mathbf{v}) d\mathbf{v}_\alpha$$

The system involves the non-dimensional parameters  $r_p \equiv R_p/\lambda_{De}$ ,  $\delta_\alpha \equiv T_\alpha/T_e$ ,  $\mu_\alpha = m_\alpha/m_e$ ,  $e_\alpha = q_\alpha/e$ ,  $\beta = n_{em0}/n_0$  and  $\phi_p$ , and the boundary conditions

$$\phi(\Gamma) = \phi_p, \quad \phi(r \rightarrow \infty) \rightarrow 0$$

$$f_{em}(\Gamma, \mathbf{v} \cdot \mathbf{u}_n > 0) = f_{HM} \equiv \frac{2}{\pi} \exp\{-(\mathbf{v} \cdot \mathbf{v})\}, \quad f_{em}(r \rightarrow \infty, \mathbf{v}) = 0$$

$$f_{e,i}(r \rightarrow \infty, \mathbf{v}) \rightarrow f_M \equiv \frac{1}{\pi} \exp\{-(\mathbf{v} \cdot \mathbf{v})\}, \quad f_{e,i}(\Gamma, \mathbf{v} \cdot \mathbf{u}_n > 0) = 0$$

being  $\mathbf{u}_n$  the normal unit vector to  $\Gamma$  taken in the outward direction.

## Results

To quantify the impact of the population of trapped particles and the role of the electron emission, we compared the solutions obtained with SVPS and CPIC for the set of non-dimensional parameters (see Fig. 1)

$$r_p = 1, \quad \delta_i = 1, \quad \mu_i = 1836, \quad \phi_p = -10, \quad \delta_{em} = 0.32, \quad \beta = \{0, 10, 30\}. \quad (3)$$

The SVPS assumes stationary conditions (i.e.,  $\partial f_\alpha/\partial \tau = 0$ ) and sets the distribution function of trapped particles to zero. On the contrary, provided an initial condition  $f_\alpha(0, \mathbf{r}, \mathbf{v}) = f_0$ , non-stationary solvers like CPIC can compute self-consistently the population of trapped particles arising during the transient. For  $\beta = 0$  (top left), we observe that, starting from an empty domain ( $f_0 = 0$ , dash-dotted blue line), the sheath resembles that predicted by the stationary solver (solid green) and no trapping is detected. However, if the initial condition corresponds to a Maxwellian plasma ( $f_0 = f_M$ , dashed magenta line), trapped particles appear and the resulting  $n_i$  profile displays a bump in the region close to the probe boundary. Therefore, the final amount of trapped particles depends on the history of the system.

Bottom left ( $\beta = 10$ ) and bottom right ( $\beta = 30$ ) panels show that the population of trapped particles increases with the emission level, with  $n_i$  becoming greater than the unperturbed plasma density away from the probe for  $\beta = 30$ . Increasing the emission level the probe enters the SCL operational regime, where a potential well develops at the probe boundary as a

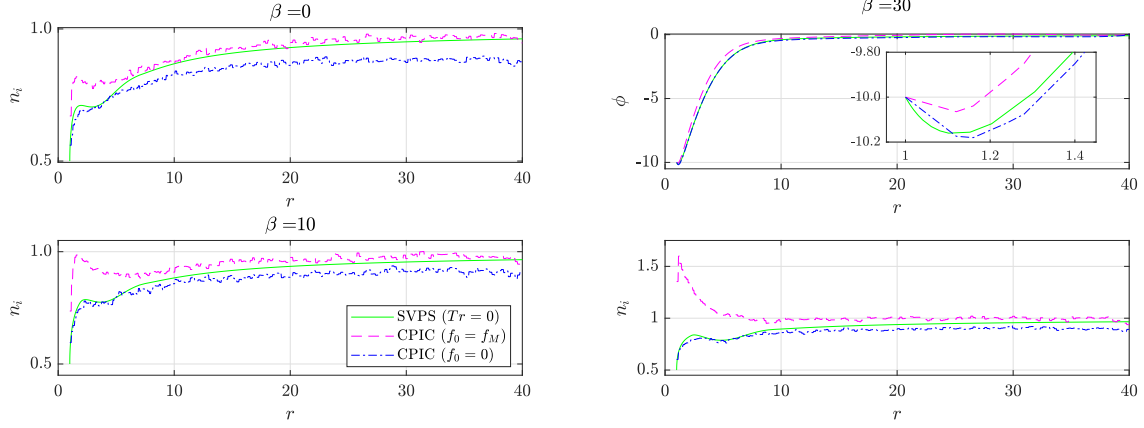


Figure 1: Density of attracted species for  $\beta = 0$  (top left),  $\beta = 10$  (bottom left),  $\beta = 30$  (bottom right). Electrostatic potential profile for  $\beta = 30$  (top right). Results shown for SVPS (solid green) and CPIC for  $f_0 = 0$  (dash-dotted blue) and  $f_0 = f_M$  (dashed magenta).

consequence of the enhanced population of emitted electrons. The inset in the top right panel in Fig. 1 shows that the presence of trapped particles makes the potential well less pronounced. As a consequence, a smaller portion of electrons is reflected back to the probe, resulting in a value of emitted current  $\approx 20\%$  bigger than without trapping.

PIC codes are widely used to investigate plasma sheaths, but are known to be affected by statistical noise induced by the macro-particles discretisation of the phase space. A free-of-noise alternative to PIC are backward semi-Lagrangian schemes like the NSVPS here presented, which is an extension of the stationary solver of Ref. [13]. The NSVPS exploits that, in a collisionless plasma, the distribution function is conserved along the characteristics of the Vlasov equation and it holds that  $f_\alpha^{n+1}(\mathbf{r}, \mathbf{v}) = f_\alpha(\tau_n + \Delta\tau, \mathbf{r}, \mathbf{v}) = f_\alpha(\tau_n, \mathbf{r}^*, \mathbf{v}^*) = f_\alpha^n(\mathbf{r}^*, \mathbf{v}^*)$ , with  $\Delta\tau > 0$  a small time step and  $(\mathbf{r}^*, \mathbf{v}^*)$  the origin of the characteristic passing through  $(\tau_{n+1}, \mathbf{r}, \mathbf{v})$ . Since  $f_\alpha^n(\mathbf{r}, \mathbf{v})$  is known, the value of  $f_\alpha^n(\mathbf{r}^*, \mathbf{v}^*)$  is computed through interpolation. A first version of the code implements a multi-linear, conservative Cloud-In-Cell interpolation method [14].

Preliminary results of the on-going verification are shown in Fig. 2, which shows a comparison between NSVPS and SVPS (solid green). For the former we carried out a sensitivity analysis varying the number of nodes in the radial dimension  $N_r$ . The NSVPS ions density profiles (left panel) are smooth as compared with those of CPIC, and higher than the one obtained with SVPS due to trapping of particles with negative (at steady-state) energy. A detailed investigation of the distribution function at the probe boundary (middle and left panels) suggests that a fine grid or a high order interpolation scheme is needed to compute  $f_\alpha$  accurately.

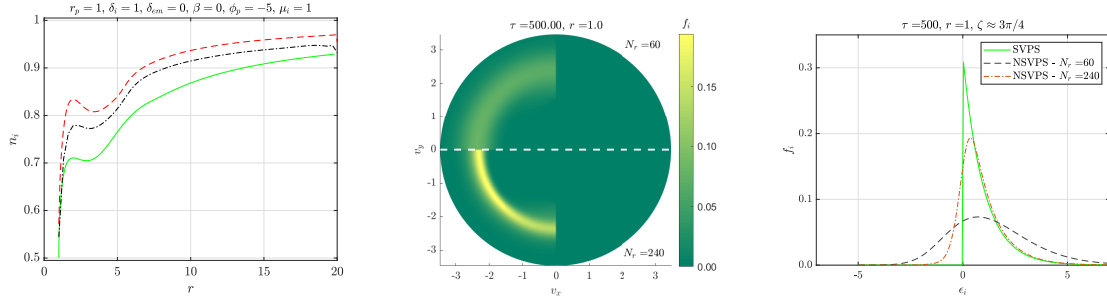


Figure 2: Plasma ions density (left), map of  $f_i(\Gamma)$  in the velocity space (middle), profile of  $f_i(\Gamma)$  for a fixed velocity angle (right). NSVPS results shown for  $f_0 = f_M$  and  $N_r = 60$  (black) and  $N_r = 240$  (red).

## Conclusions

The present work discussed the role of particle trapping in the sheath around two-dimensional electron-emitting objects in Maxwellian plasmas. A comparison between the results of a stationary Eulerian solver and a PIC code showed that the final trapped population depends on the transient. A parametric analysis investigating the sheath for different values of emission levels showed that electron-emission enhances the population of trapped particles, which, in turn, opposes the onset of the SCL regime and mitigates its effect on current emission. Preliminary results obtained with a novel backward semi-Lagrangian solver were discussed as well.

## Acknowledgement

This work was supported by the European Union's Horizon 2020 Research and Innovation Programme under grant agreement No 828902 (E.T.PACK project).

## References

- [1] A. V. Gurevich, *Sov. J. Exp. Theor. Phys.* **26** 575 (1968)
- [2] M. Lampe et al., *Physics of Plasmas* **10**, 1500-1513 (2003)
- [3] M. Shoucri et al., *Eur. Phys. J. D* **30**, 81–92 (2004)
- [4] F. Taccogna et al, *Physics of Plasmas* **13**, 043501 (2006)
- [5] G. Sánchez-Arriaga, *Physics of Plasmas* **20**, 1 (2013)
- [6] A. A. Kiselyov et al, *EPL* **111**, 1 (2015)
- [7] V. L. Krasovsky and A. A. Kiselyov, *IEEE Transactions on Plasma Science* **46**, 3 (2018)
- [8] B. F. Kraus and Y. Raitses, *Physics of Plasmas* **25**, 030701 (2018)
- [9] G. R. Johnson and M. D. Campanell, *Plasma Sources Science and Technology* **30**, 1 (2021)
- [10] X. Chen, G. Sánchez-Arriaga, *Physics of Plasmas* **24**, 2 (2017)
- [11] G. L. Delzanno et al., *IEEE Transactions on Plasma Science* **41**, 12 (2013)
- [12] G. L. Delzanno and X. Tang, *Physics Review Letters* **113**, 3 (2014)
- [13] L. Chiabò and G. Sánchez-Arriaga, *Journal of Computational Physics* **438**, 110366 (2021)
- [14] Birdsall, Charles K. and Langdon, A. Bruce, *Plasma physics via computer simulation*, Taylor and Francis, (2005)